FINITE ELEMENT SIMULATION OF BLAST LOADING ON SANDWICH STRUCTURE WITH FACE PLATES OF CERAMIC

M.Tech. Thesis

By

ROHAN DEWDA

DISCIPLINE OF MECHANICAL ENGINEERING

INDIAN INSTITUTE OF TECHNOLOGY INDORE

JUNE 2024

FINITE ELEMENT SIMULATION OF BLAST LOADING ON SANDWICH STRUCTURE WITH FACE PLATES OF CERAMIC

A THESIS

Submitted in partial fulfillment of the requirements for the award of the degree
of
Master of Technology

by

ROHAN DEWDA

DISCIPLINE OF MECHANICAL ENGINEERING

INDIAN INSTITUTE OF TECHNOLOGY INDORE

JUNE 2024

INDIAN INSTITUTE OF TECHNOLOGY INDORE

CANDIDATE'S DECLARATION

I hereby certify that the work which is being presented in the thesis entitled **FINITE ELEMENT SIMULATION OF BLAST LOADING ON SANDWICH STRUCTURE WITH FACE PLATES OF CERAMIC** in the partial fulfillment of the requirements for the award of the degree of **Master of Technology** and submitted in the **Discipline of Mechanical Engineering, Indian Institute of Technology Indore,** is an authentic record of my own work carried out during the time period from July 2022 to June 2024. Thesis submission under the supervision of **Dr. Indrasen Singh**, Assistant Professor in Mechanical Engineering Department, Indian Institute of Technology Indore.

The matter presented in this thesis has not been submitted by me for the award of any other degree of this or any other institute.

28/6/2024

ROHAN DEWDA
(M.Tech. Student)

This is to certify that the above statement made by the candidate is correct to the best of my knowledge.

29-06-2024

Dr. Indrasen Singh
(Thesis Supervisor)

Rohan Dewda has successfully given his M.Tech. Oral Examination held on **30 May 2024**.

29-06-2024

Signature of Supervisor of M.Tech. thesis
Date:

Convener, DPGC
Date: 01-07-2024

ACKNOWLEDGEMENTS

I am very thankful to INDIAN INSTITUTE OF TECHNOLOGY INDORE for providing me the opportunity and facilities to carry out my work. I would like to express my sincere gratitude to my supervisor Dr. Indrasen Singh for providing me the opportunity to work on this interesting problem. I would also like to thank him for his constant support and help throughout the duration of my stay at the institute, I am very grateful to him for teaching me from tiny concepts to the bigger concepts in subjects like theory of elasticity, Finite Element methods, and Fracture Mechanics.

I am very much thankful to my friend and colleague Miss Mahima Yadav for giving me assistance in learning ABAQUS explicit Coupled Eulerian and Lagranian technique for the near field blast simulations. I am grateful to my dear beloved seniors Mr. Ramanand Dadhich and Mr. Sumit Chorma for their constant support in solving the problems encountered during my project, and also assisting me to work in the correct direction. I am delighted to show my gratitude towards Mr. Arun Singh and Mr. Manik Bhowmik for providing emotional support throughout the journey of my master thesis.

I also express my deep gratitude towards my parents: Shri Subhash Dewda and Shrimati Pinky Dewda, grandparents: Shri Babulal Dewda and Shrimati Sitabai Dewda & Shri kailash Verma and Shrimati Kalawati Verma, and sister: Miss Chitranshi Dewda for their love and continuous encouragement to do better in my life. I would also like to thank my dear friends Mr. Siddhant Jain and Mr. Sanyam Jain for believing in me and motivating me to get better every day.

Dedicated to

My parents

Shrimati Pinky Dewda & Shri Subhash Dewda

Abstract

The threat from bomb blast like landmines, improvised explosive devices, mortars cause most of the injuries in battlefield. Foot being in closest proximity with ground suffers majority of injuries in case of a landmine blast. Therefore, a protective measure is needed to ensure safety of lower portion of the body. For this purpose, various blast resistant structures such as monolithic steel plates, sandwiched corrugated plates, sandwich metallic foams, sandwich honeycomb structure have been developed to mitigate the effects of blast wave. Among them, the sandwich honeycomb structure which are comprised of a soft metallic core sandwiched between two metallic plates have been preferred over other structures due to their light weight and high energy absorption capability. The experiments on ceramics have shown that these materials are more effective for attenuation of pressure wave than metals. Therefore, it is advisable to combine ceramic plates with soft honeycomb sandwich structure. Though a few efforts have been made in this direction, a systematic study is still needed to understand the effect of the addition of ceramic plate on the blast resistant characteristics of a sandwiched structures. Therefore, the finite element simulations of near field blast loading on honeycomb sandwich structure with and without ceramic plate attached are performed. Results show that inclusion of ceramic plates on sandwiched structures results in better pressure attenuation and energy absorption.

TABLE OF CONTENTS

LIST OF FIGURES

LIST OF TABLES

NOMENCLATURE

Symbols:

A	Yield Stress
B	Work hardening coefficient
C	Strain rate sensitivity coefficient
D	Damage parameter
$\dot{D}$	Rate of damage
d	Standoff distance
n	Work hardening exponent
m	Thermal softening exponent
SD	Scaled distance
T	Actual temperature
T_r	Room temperature
T_m	Melting temperature
W	Mass of TNT

Greek letters:

σ_i^*	Normalized intact strength with respect to HEL

σ_f^*	Normalized fracture strength with respect to HEL
P^*	Normalized pressure with respect to HEL
T^*	Normalized tensile pressure with respect to HEL
σ_{HEL}	Hugnoit limit
ω	State variable
L_{eq}	Characteristic length
$\underline{u}_f^p$	Plastic displacement at failure
η	Triaxilality
$\in_f^p$	Plastic strain at failure
σ_{eq}	Equivalent stress
$\in_p$	Equivalent plastic strain
$\dot{\in}_p$	Strain rate
$\dot{\in}_o$	reference strain rate

ACRONYMS

IED	Improvised explosive devices
PVC	Polyvinyl chloride
HSS	Honeycomb sandwich structure
CEL	Coupled eulerian and lagrangian technique
JH2	Johnson Holmquist model 2
J-C	Johnson Cook
TNT	Trinitrotoluene
HEL	Hugnoit elastic limit
EC3D8R	Explicit Continuum 3D 8-node Reduced Integration
C3D8R	Continuum 3D 8-node Reduced Integration
S4R	Shell 4-node Reduced Integration

Chapter 1

Introduction and Literature Review

1.1 Introduction

Threats from ongoing terrorist activities, wars between nations, and the Naxalite insurgency are not a new concern to deal with. Research on the development of protective equipment like bulletproof jackets for bullets, fragmentation vests, advanced combat helmets, ballistic goggles, and blast-resistant boots for mortars, landmines, and Improvised Explosive Devices (IEDs) are the main areas of interest and concern. The foot, being in closest proximity to the ground suffers the majority of injuries in case of a landmine blast, and thus it requires special attention to ensure the safety of the lower portion of the body from the blast wave; preventing lethal leg and spine injuries, causing handicap, paralysis, limb amputation , and even death. Although many blast-resistant structures like monolithic steel plates, sandwiched corrugated plates, sandwich metallic foams, and sandwich honeycomb structures have been developed to mitigate the effects of the blast wave. However, due to the continuous increase in the amount of explosives in mortars, IEDs, and landmines, there remains a need to improve blast-resistant structures to mitigate the effects of the blast wave by enhancing energy absorption, pressure attenuation, reducing maximum deflection, limiting jerk, and damping vibrations. Among blast-resistant structures, the sandwich honeycomb structure which is comprised of a soft metallic core sandwiched between two metallic plates has been preferred over other structures due to its light weight and high energy absorption capability. The experiments on ceramics have shown that these materials are more effective for the attenuation of pressure waves than metals. Therefore, it is advisable to combine ceramic plates with a soft honeycomb sandwich structure to increase the blast resistance of the structure. In view of the above considerations, finite element simulations of near-field blast loading on a honeycomb sandwich structure with and without a ceramic plate attached are performed in this thesis. In addition, a structure completely made of ceramic material is also analyzed and compared with an aluminum sandwich honeycomb structure with and without a ceramic plate. The relevant background is briefly presented below.

1.2 Landmine

Landmines are explosive devices that might be activated by pressure (the weight of a human or a vehicle), tripwires, or proximity sensors. Generally, these explosive devices are camouflaged under the soil to prevent any enemy from entering the territory (refer Fig. 1.1). There are two types of landmines: anti-personnel landmines, designed to harm an individual who comes in proximity to the landmine, and anti-tank landmines, designed to target armored vehicles, which require much higher pressure to activate. Nowadays, landmines are also laid by terrorist organizations to harm military forces and civilians. Anti-personnel mines can cause severe injuries, including eye injuries, shrapnel wounds, hearing loss, burns, muscle tears, and amputations, even causing fatalities. The body part that is closest in proximity to the landmine is the lower limb, causing severe damage to it. Therefore, studying the effect of anti-personnel landmines on the lower limb is essential to finding ways to reduce the severity of injuries.

Fig. 1.1 Landmine clearers showing landmines recovered from the site [1].

1.3 Landmine blast explosion on human leg

Explosion are one of the main cause of deaths in the war zone, activation the explosive forms an outward propagating blast wave causing rapid pressure rise and deformation, the pressure gradually decreases with time and distance after passing through maxima called as peak pressure, after a positive phase of wave a negative phase is developed and vacuum is generated, these time history of pressure is known Friedlander wave [2]. Being in contact with the ground, the lower limb experiences the majority of injuries in a landmine blast, typically accounting for 54% of battle wounds [3, 4]. The injuries consist of tibia fracture, fibula fracture (refer Fig. 1.2), compartment syndrome etc. About 32.4 % victims dies immediately after the landmine blast and rest 67.6 % survived the permanent injuries [5]. It has been observed that these injuries are directly linked to peak overpressure [6] and numerous studies have been done to investigate critical pressure to cause these injuries. According to published research, the minimum tibia axial force to cause is approximately 6-8 KN [6, 7]. Several Structures have been effectively developed for reducing the peak pressure, such as monolithic steel plate [8], ceramics [9], sandwiched corrugated plates [10], sandwich metallic foams [11], and sandwich honeycomb structure [12]. But due to the increase in mass of explosives in landmines, it is necessary to do regular improvements in the existing blast resistant structures or redesigning the structures to attenuate the peak pressure and absorbs energy associated to blast wave. The most commonly used sandwiched structures for application of blast resistance are discussed in the following section.

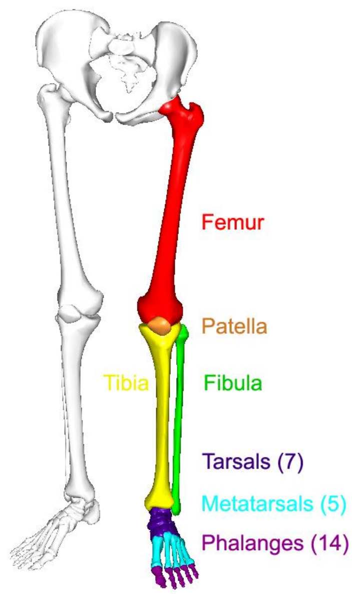

Fig. 1.2 Schematic representing basic anatomy of human leg [13].

1.4 Sandwich Structure

Various experimental and theoretical analyses have been done to mitigate the effects of blast waves, lightweight sandwich structures which comprised of soft core sandwiched between two metallic backing plates, can deform heavily under compressive loading, absorbing significant amount of energy associated with the blast wave by means of plastic deformation, also these structures possess higher bending strength and outperforms monolithic structures significantly hence could be a potential candidate for blast resistance application [13-15] , serving the purpose of energy absorption and impact effects mitigation. The idea behind the use of sandwich structure is to combine the advantage of stiffness and strength of thin face sheets and lightweight of thicker flexible core to accomplish preeminent structural properties. Typical design of a sandwich structure is shown in Fig. 1.3, and the components of sandwich structure are discussed briefly in the following section.

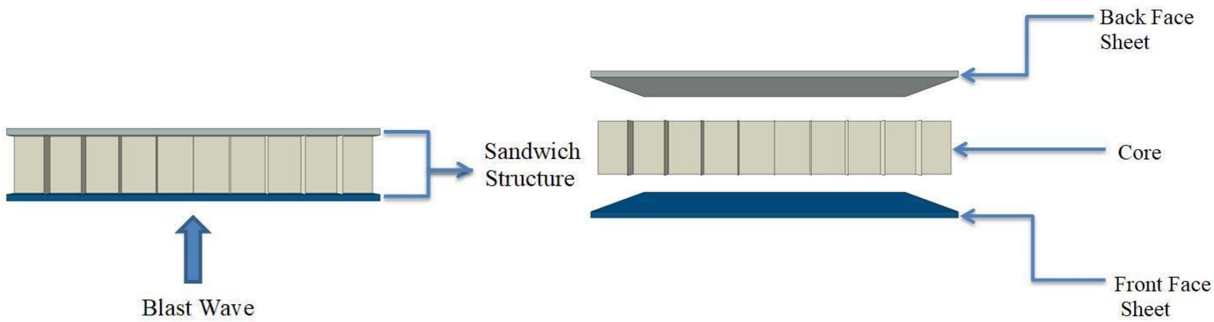

Fig. 1.3 Schematic showing the sandwich structure and its components.

1.4.1 Face Sheets

There are various roles associated to the face sheets in sandwich structure, from providing bending stiffness and structural integrity to the structure, to acting as barrier to fragments and debris formed during the explosion, also the key function of face sheets is to distribute load evenly across the core which helps in achieving more uniform deformation and enhanced energy absorption capabilities. There are typically two types of face sheets in these structures: the front face sheet and the back face sheet, each serving distinct purposes:

- **Front Face sheet:** The face sheet facing the blast is generally known as front face sheet (refer Fig. 1.3), the front face sheet is designed to evenly distribute the applied load across the entire cross-section. This uniform distribution of the load minimizes the localized deformation of the core and thereby promoting uniform deformation of the core and hence enhancing the energy absorbing capability of the structure. It also prevents shrapnel and hot gases from breaching the core and critical areas of personnel. Additionally, the front face sheet acts as a protective shield against the shrapnel and hot gases from breaching the critical areas of the personnel.

- **Back face sheet:** The face sheet opposite to the blast side, backed at another side of core is known as back face sheet (refer Fig. 1.3). The back face sheet provides structural integrity and bending stiffness to the sandwich structure, regulating the back face deflection, and preventing the fragments formed during crushing of core, from penetrating into the foot of personnel.

1.4.2 Core

The thick low density layer sandwiched between the two face sheets is known as core (refer Fig. 1.3), due to its soft nature, core provides minimal resistance to deformation, allowing it to deform easily under compressive load, and attenuate the pressure associated with the blast wave, additionally the core absorbs significant amount of energy associated with blast wave by the means of plastic deformation and compression of air entrapped inside cells under compressive loading conditions. There are different types of core used in various applications, discussed briefly in the following section.

- **Polymeric Foam cores:** These foams are made up of polymers like polyurethane, polystyrene, PVC foams etc. These lightweight foams provide decent strength to weight ratio, and can absorb significant energy. Polymeric foams are good insulators and can prevent heat transfer from blast wave to foot. Also the manufacturing of polymeric foams is relatively easier.
- **Metallic Foam cores:** Metallic foams provide very high strength to weight ratio making them lightweight and high strength structures making them suitable for blast resistance application, although the manufacturing of metal foams is a relatively tougher job.
- **Metallic honeycomb cores:** Metallic honeycomb cores are mostly used structures for applications under dynamic loading, these structures consist of cells of different shapes and sizes, oriented perpendicularly to the loading direction (out of plane loading), or they may be oriented parallel to the direction of loading (known as in-plane loading) The name honeycomb derives from the hexagonal

honeycomb structure inspired by a beehive, which is known for its structural strength.

Among the above core types, honeycomb structures are preferred over others due to their versatility in customizing properties through adjustments in cell shape, size, cell wall thickness, and orientation within the honeycomb configuration, all tailored to meet specific design objectives of the structure. Although the sandwiched honeycomb structures are effective blast resistant structures and are optimized significantly, further modification and improvements need to be implemented in the structure to withstand the larger masses of explosives.

1.5 Review of pertinent literature

1.5.1 Blast mitigating structures

Various structures have been designed and developed to mitigate the effect of blast wave, from the simplest being the monolithic steel plate [18] to more sophisticated structures like steel-ceramics composite [19], sandwiched corrugated plates [20], sandwich metallic foams [21], sandwich honeycomb structure [12, 14, 15, 18, 19, 21-24]. Among them, the sandwich honeycomb structures have been preferred over other structures due to their light weight and high energy absorption capability.

1.5.2 Deformation behavior of sandwich honeycomb structure

Dharmasena et al. [14] showed that the honeycomb sandwich structures (HSSs) exhibit higher energy absorption and lower back face deflection than monolithic structures of identical materials. Theobald et al. [22] showed that thicker core of honeycomb in sandwich structure is better as it leads to greater blast resistance. They also showed that the honeycomb core performs better than aluminum foam panels. Different materials for honeycomb's core have also been explored to achieve enhanced blast resistant characteristics [23]. For instance, Karagiozova et al. [23] demonstrated that aluminum HSSs outperformed polystyrene HSSs in reducing initial pressure pulses. Numerous researchers have contributed to the development of blast resistant materials by studying the effect of geometrical and material parameters on the strength and efficiency of structures [12, 14, 22, 24, 25]. Qi et al. [26] found out that the use of material with lower stiffness in front face sheet results in higher energy absorption, while material with high stiffness used in back face sheet results in lower back face deflection. Apart from studying the effect of materials on front and back face sheets, the effect of inclusions of additional layers have also been investigated. For example, Yehia A. et al. [27] found that inclusion of polyethylene elastomeric foam between AS4/3501-6 carbon/epoxy face sheet and H100 Divinycell foam core increased the blast resistance of sandwich panels. The experiments evidences shows decrease in back face deflection with increase in front face thickness and core thickness [24]

Thomas and Tiwari [12] studied the effect of geometrical parameters of sandwich honeycomb structure like cell wall thickness, face sheet thickness, cell size, core thickness, and standoff distance subjected to air blast. A very detailed study on sandwich honeycomb structures has been conducted to investigate the effects of shape of cells, cell size, cell wall thickness on the performance of sandwich honeycomb structures [8-15, 22-24]. Also, the effect of material and thickness of face sheets have been investigated for sandwich honeycomb structures [26]. The structures with negative poisson's ratio, famously known as auxetic structures are also studied for blast applications and are found to be effective, because of experiencing uniform deformation under blast loading due to negative poisson's ratio effect [28,29]. Also, Xiaochao Jin et al. [30] showed that the graded honeycombs i.e. multiple layered honeycombs are better than the monolayer honeycombs in both energy absorption and back face deflection considerations.

1.5.3 Deformation Behavior of Ceramics

Ceramics are very effective as armor in anti-ballistic applications like in tanks, armor, engine parts etc. [19, 25, 31-37] due to their high strength, hardness, and low density. Ceramic as an anti-ballistic has been studied widely by research scholars over years [19, 25, 31-37], but very fewer efforts are made to study the ceramics under blast. Due to high energy absorbing capacity, there lies a potential to use ceramics under blast loading applications [38, 39]. Changel Zhang et al. [19] aimed to study the damage characteristics of ceramic composite structures under explosive loading through experiments and finite element modeling. They found that ceramic composite structures; ceramic sandwiched between glass fibers with backing plate of steel, are found to be more effective than structures without ceramic plates, as ceramic exhibits robust wave-weakening ability, while the steel back plate absorbs a major portion of detonation energy. Alumina (AD99) and silicon carbide (SiC) ceramics display similar anti-detonation performance at matched surface densities, with distinct fracture mechanisms, AD99 failing predominantly by intergranular fracture, while SiC failed by transgranular fracture. [19].

1.6 Issues for investigations

Sandwich structures subjected to blast loading are studied in detail and are optimized significantly. Ceramic materials such as silicon carbide, alumina etc., although possessing desired properties for the blast wave mitigation such as energy absorption, robust wave-weakening ability, have not been studied much under the case of blast loading, very few investigations have been done to understand the behavior of ceramic under blast [25]; investigating the behavior of ceramics under blast could lead to promising results for the application of blast resistance and hence necessitate to undertake a study of ceramics subjected to blast loading.

1.7 Objectives and scope of thesis

It can be noticed from the above discussion that the experiments on ceramics have shown that these materials are more effective for attenuation of pressure wave than metals. Therefore, it is advisable to combine ceramic plates with soft honeycomb sandwich structure. Though a few efforts have been made in this direction, a systematic study is still needed to understand the effect of the addition of ceramic plates on the blast resistant characteristics of sandwiched structures. Therefore, the finite element simulations of near field blast loading on honeycomb sandwich structure with and without ceramic plate attached are performed. Additionally, the structure completely made up of ceramic material is also simulated, analyzed, and compared with the honeycomb sandwich structure with and without ceramic plate attached. The study aims to find the optimum structure for the application of blast loading.

1.8 Organization of thesis

The remaining portion of the thesis is organized as:

In chapter 2, the modeling strategy to simulate the behavior of structure under near field blast loading is discussed in detail which covers introduction to near field blast, constitutive models used for simulation, the coupled Eulerian-Lagrangian technique is discussed, subsequently the finite element model is elaborated.

The Chapter 3 consists of the observations, results, and discussion of the simulation performed in chapter 2, finally the important results and possible future work are also summarized.

Chapter 2

Development of finite element model

2.1 Introduction

This chapter covers the comprehensive modeling strategy employed to simulate the deformation behavior of sandwich structures subjected to near field blast loading. The chapter begins with introducing near field blast discussed in Sec. 2.2, followed by the thorough description of the material models utilized in the simulations including stress-strain response, damage evolution, and nonlinear characteristics. The coupled Eulerian-Lagrangian simulation technique (CEL), an advanced technique that combines the strengths of Lagrangian and Eulerian framework enabling effective capturing of parameters under complex interactions between blast wave and structural components is described in Sec. 2.4. Finally, the material properties, and the finite element model of structures is described in Sec. 2.5 and Sec. 2.6 respectively. The geometry, mesh generation strategy, boundary conditions and loading scenarios used for simulations are discussed briefly in section 2.5.1.

2.2 Near field blast

The quantification of a blast on a structure is generally described by the parameter derived using empirical relationship known as scaled distance, SD. The idea behind the above differentiation between near field and far field blast is that even a smaller amount of explosive can cause significant damage if detonated very close to the structure. Additionally, the effects of a larger mass of explosive cannot be felt at a greater distance. Considering the above discussion, the empirical relation of scaled distance is given as [40].

$$SD = d/\sqrt[3]{W} \tag{2.1}$$

Where, d is the distance between the point of interest and the point of detonation in meter, and W is mass of explosive $in\ kg$. If the scaled distance is less than 1.18 then the blast is considered near field blast [41], otherwise, it is considered as far field blast. The loading conditions taken for consideration in the thesis falls in the category of near field blast loading.

2.3 Constitutive models

The dynamic mechanical behaviors of honeycomb core made of ceramic and soft material like Aluminum are compared to choose a suitable material for anti-mine boot application. In this study, the deformation behavior as well as damage in Aluminum is assumed to be characterized by Johnson-Cook constitutive law (JC) and Johnson-Cook damage law [42]. However, the ceramic (SiC) is assumed to follow Johnson Holmquist model 2 (JH2) model [43]. These models are described briefly in the following.

2.3.1 Johnson-Cook Plasticity Theory

The typical stress-strain diagram for ductile material is shown in Fig. 2.1. The elastic region is assumed to follow Hooke's law (O-A), after that the flow stress is assumed to follow Johnson-Cook plasticity (A-C) and damage (B-C) is assumed to follow Johnson-Cook damage model.

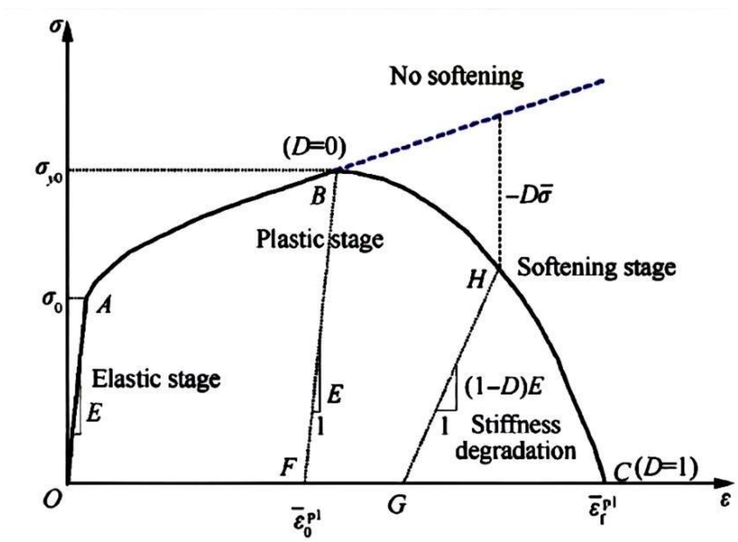

Fig. 2.1 Typical stress-strain diagram of ductile material (reproduced from Hu and Zhang, 2019 [44]**).**

The equivalent stress, σ_{eq} in Jonson Cook model is considered to evolve as:

$$\sigma_{eq} = \left[A + B\left(\epsilon_p\right)^n\ \right] \times \left[1 + Cln\left(\frac{\dot{\epsilon_p}}{\dot{\epsilon_o}}\right)\right] \times \left[1 - \left(\frac{T - T_r}{T_m - T_r}\right)^m\right]. \qquad \textbf{(2.2)}$$

Here, the ϵ_p, $\dot{\epsilon_{p}}$, and $\dot{\epsilon_o}$ are plastic strain, plastic strain rate, and reference strain rate respectively. Further, T is actual temperature, T_r is room temperature, and T_m represent melting temperature. Further, the parameters A, B and C are material constants representing yield strength of the material, work hardening coefficient of material and strain rate sensitivity coefficient, respectively. Moreover, the constants n and m are work hardening exponent and thermal softening coefficient, respectively.

2.3.2 Johnson-Cook Damage Model

To simulate the failure in Aluminum, the Johnson-Cook damage model is invoked which is governed by the following equation:

$$\epsilon_{\mathrm{f}}^{\mathrm{p}} = [D_1 + D_2 e^{-D_3 \eta}] \times \left[1 + D_4\, ln\, ln \left(\frac{\dot{\epsilon}_p}{\dot{\epsilon}_o}\right)\right] \times \left[1 + D_5 \left(\frac{T - T_r}{T_m - T_r}\right)\right]. \quad \textbf{(2.3)}$$

In the equation 2.3, the constants $D_1 - D_5$ are known as damage parameters, while $\epsilon_{\mathrm{f}}^{\mathrm{p}}$ is equivalent strain at failure. Further $\eta = \frac{\sigma_H}{\sigma_{eq}}$ is stress triaxiality, where σ_H represent hydrostatic stress. The damage in material is assumed to start when the state variable ω reaches the value unity, defined as:

$$\omega = \int \frac{d \in^p}{\epsilon_{\mathrm{f}}^{\mathrm{p}}(\eta, \dot{\in^p})}. \quad \textbf{(2.4)}$$

After damage initiation, the stiffness, σ, of the element which has started failing is assumed to degrade as:

$$\sigma = (1 - D)\sigma_{eq}. \quad \textbf{(2.5)}$$

Where the parameter D is known as damage parameter which is assumed to evolve from zero to unity following the given damage evolution law:

$$\dot{D} = \frac{(L_{eq}\, \dot{\in_p})}{\underline{u}_f^p}. \quad \textbf{(2.6)}$$

Where, L_{eq} represents the characteristic length of the element and $\underline{u}_f^p$ is the effective plastic displacement at complete degradation/failure.

2.3.3 Johnson and Holmquist model-2 (JH-2)

Brittle materials like silicon carbide are modeled using Johnson-Holmquist Model-2 material model. These materials contain inherent flaws like triple junctions, weak grain boundaries, inclusions, second phases, pores etc. inside them which get triggered upon loading and act as stress concentration sites. Under loading conditions, the crack tip experiences the stress field at the crack tips, causing the propagation of crack above critical limit of stress, further the propagation of cracks leads to merging of different cracks causing material stiffness degradation, when acted by the tensile force, the single crack propagates predominantly and ultimately leads to catastrophic failure of material. As on application of compressive load the material experiences closing of cracks, which results in enhancement of strength of the material, therefore unlike ductile materials the brittle materials are pressure sensitive solids and the strength of material depends upon both, the amount of damage the materials has undergone as well as the hydrostatic pressure experienced by the material as shown in Fig. 2.2.

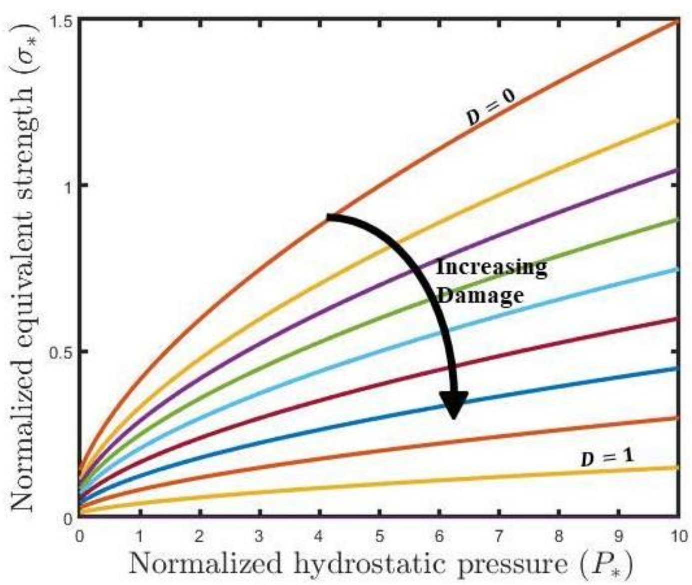

Fig. 2.2 The variation of strength with respect to pressure at different damage levels in a brittle material. The curves obtained by plotting σ^* versus P^* in Eq. 2.7, Eq. 2.8, and Eq. 2.9 in JH2 model.

The JH-2 Model considers the normalized strength of material as a function of both damage and hydrostatic pressure experienced by material. In JH2 model, the normalized equivalent stress, $\sigma^* = \sigma/\sigma_{HEL}$, ($\sigma_{HEL}$ being strength at Hugnoit elastic limit) in a brittle material is considered to evolve as:

$$\sigma_* = \sigma_i^* - D\left(\sigma_i^* - \sigma_f^*\right). \quad \textbf{(2.7)}$$

Here, σ_i^*, and σ_f^* are the strength of intact solid and damaged solid and are named as intact and fractured strength, respectively. These are defined as:

$$\sigma_i^* = A(P^* + T^*)^N(1 + C\ ln\ ln\ \epsilon^*\ ), \quad \textbf{(2.8)}$$

and,

$$\sigma_f^* = B(P^*)^M(1 + C\ ln\ ln\ \epsilon^*\ ). \quad \textbf{(2.9)}$$

In Eqs. (2.8) and (2.9), the parameters$A$, B and C are normalized intact yield strength, normalized fractured yield and strain rate sensitivity coefficient, respectively. Further, T^*, and P^* represent temperature and pressure normalized by corresponding quantities at Hugnoit elastic limit. Moreover, ϵ^* in Eq. (2.8) and (2.9) is normalized strain in solid. The damage parameter D in Eq. (2.7) is defined as:

$$D = \frac{\sum \Delta\epsilon^p}{\epsilon_f^p}. \quad \textbf{(2.10)}$$

Where, ϵ^p is equivalent plastic strain and ϵ_f^p is plastic strain at failure.

2.4 Coupled Eulerian-Lagrangian technique

A coupled Eulerian-Lagrangian (CEL) approach is employed to simulate the deformation behavior of structure under near field blast loading, so that the effect of reflected waves can be captured. The CEL simulation technique is a computational method used primarily in fluid dynamics and structural mechanics to model problems involving interactions between a fluid and solid objects within it. The Eluerian and Lagrangian frameworks are described briefly in the following section.

2.4.1 Eulerian Framework

The Eulerian approach focuses on analyzing the properties at a fixed point with respect to time, for which it involves using a fixed grid to discretize and solve the governing equations of fluid flow as shown in Fig. 2.3 (b). In this framework, the fluid properties (velocity, pressure, etc.) are defined at fixed points in space and time, regardless of whether there are solid objects present in the flow.

2.4.2 Lagrangian Framework

The Lagrangian approach involves tracking individual objects or particles (often solid bodies) as they move under deformation. Thus, it involves mesh which deforms with material as shown in Fig 2.3 (a). In this framework, the equations of motion are solved for each individual object, accounting for its position, velocity, and other relevant parameters as it interacts with the surrounding.

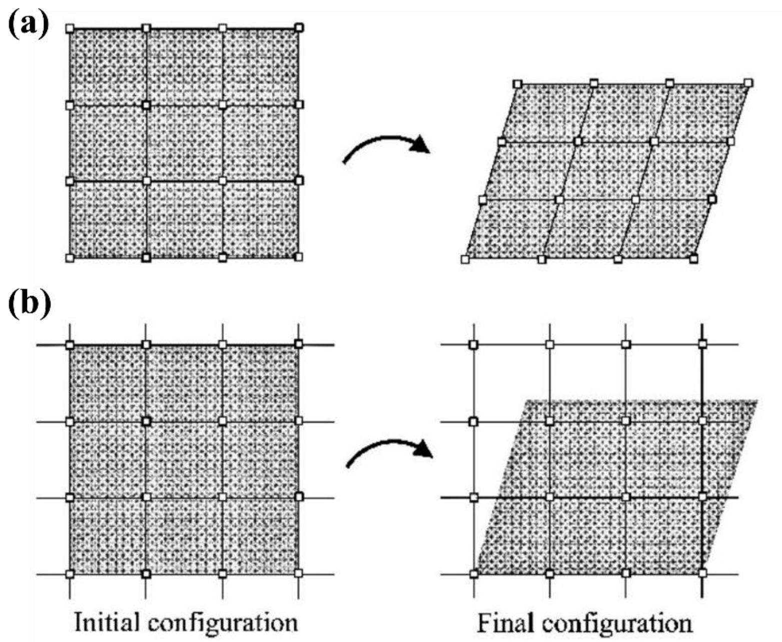

Fig. 2.3 Schematic (a) representing lagrangian based mesh and schematic (b) representing eulerian based mesh (reproduced from Colom and Alba, 2015 [45]).

The CEL technique integrates both Eulerian and Lagrangian frameworks within a single simulation. It allows for the simultaneous simulation of fluid dynamics (Eulerian) and the dynamics of solid bodies or particles (Lagrangian) that move within the fluid. This coupling is essential for accurately capturing the interactions between the fluid flow and the solid objects. The technique typically involves:

1. **Eulerian Solver:** Solving the fluid flow equations on a fixed computational grid to compute fluid properties like velocity, pressure, and temperature.

2. **Lagrangian Solver:** Tracking the motion and deformation of solid objects or particles within the fluid using equations of motion, considering forces like drag, buoyancy, and other fluid-solid interaction forces.
3. **Interaction Handling:** Exchanging information between the Eulerian and Lagrangian solvers to ensure that the forces and boundary conditions on both fluid and solid sides are appropriately accounted.

CEL is commonly used in problems where the interaction between the fluid flow and solid structures is significant, such as in aerodynamics (aircraft wings), hydrodynamics (ships), biomechanics (blood flow in arteries), and automotive engineering (vehicle), and effect of blast wave on structures. The other techniques like conventional weapon method, smooth particle hydrodynamics can capture the effect of far field blast on a structure to a considerable accuracy, but they are unable to capture the behavior of structure under near field blast accurately. The scenario of near field blast on a structure can only be accurately captured using the CEL technique and hence chosen to carry out the finite element simulations [46, 47].

2.5 Finite Element modeling

A coupled Eulerian-Lagrangian approach is employed to simulate the deformation behavior of structure under near filed blast loading, so that the effect of reflected wave can be captured. For this purpose, a cubical domain ($600\ mm \times 600\ mm \times 600\ mm$) is discretized using Eulerian EC3D8R elements available in commercially available software package Abaqus 2017. The domain comprise of air ($600\ mm \times 600\ mm \times 300\ mm$) in upper half, soil ($600\ mm \times 600\ mm \times 300\ mm$) in the lower half, and TNT ($38\ mm \times 38\ mm \times 38\ mm$) buried inside the soil at the depth of $25\ mm$ from air-soil interface, the properties of air, soil and TNT are assigned to domain using predefined fields in material assignment option of commercially available software package Abaqus 2017. The regions in the domain for TNT, air and soil are shown in schematic shown in Fig. 2.4 (a). The volume of the region for TNT is determined corresponding to its weight of 90 g.

2.5.1 Boundary conditions

Domain: The bottom surface of the domain is assumed to behave as a reflecting surface and it is also constrained to move in all the directions (refer Fig 2.4(b)), while the other outer surfaces of the domain are provided with outflow nonreflecting condition refer Fig 2.4(b)). Note that the outflow boundary conditions allow the blast wave and other flow variables to exit the computational domain smoothly, while non-reflecting boundary conditions are designed to prevent artificial reflections of blast waves at the boundaries, ensuring that the simulation accurately represents an open or infinite domain.

Structure: The structure under consideration is designed to attenuate pressure and absorb energy associated with the blast wave. Each node of the top surface is roller supported and are constrained to move in z direction as shown in Fig. 2.5. The reactions forces at each node are extracted, summed, and divide by cross-sectional area to determine the average pressure exerted on the top surface.

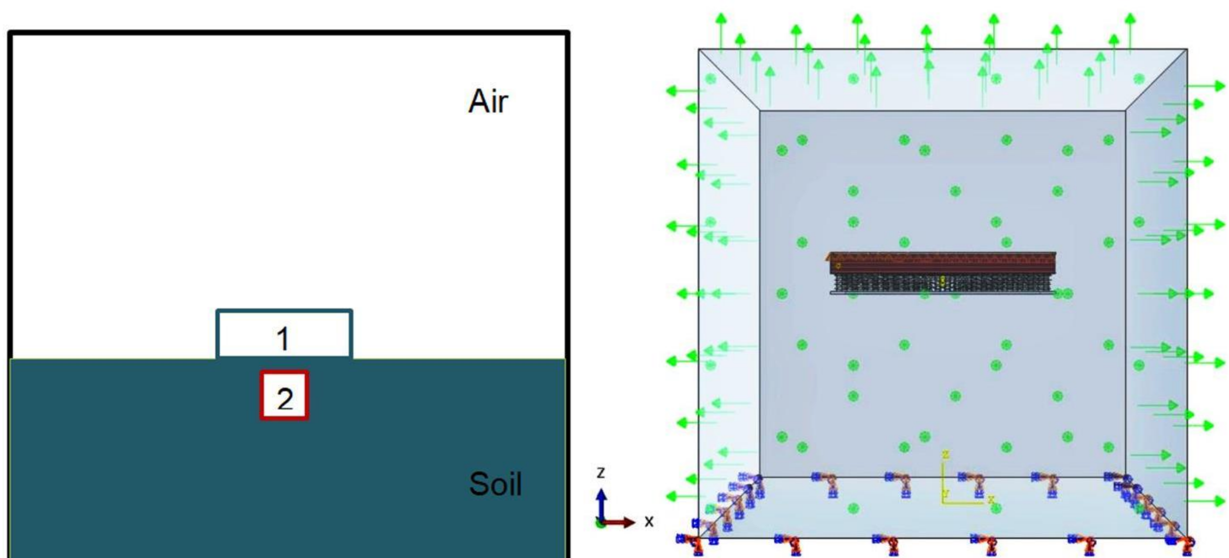

(a) (b)

Fig. 2.4 Schematic showing modeling strategy employed for simulation; (a) Schematic of model used for simulating landmine blast on a structure; (b) Abaqus model.

2.5.2 Description of structure

As displayed in Fig. 2.5 is metallic/ceramic structure under consideration which is modeled by employing three dimensional brick and shell Lagrangian elements. In this study, two types of structures are considered. In the first study, finite element simulations of blast loading on a ceramic plate, which is discretized using C3D8R elements, is performed. In the second study, the deformation behavior of honeycomb sandwiched structure is analyzed. In this case, Lagrangian S4R elements are used to model honeycomb cells, while the plates of sandwich structure are modeled by Lagrangian C3D8R elements.

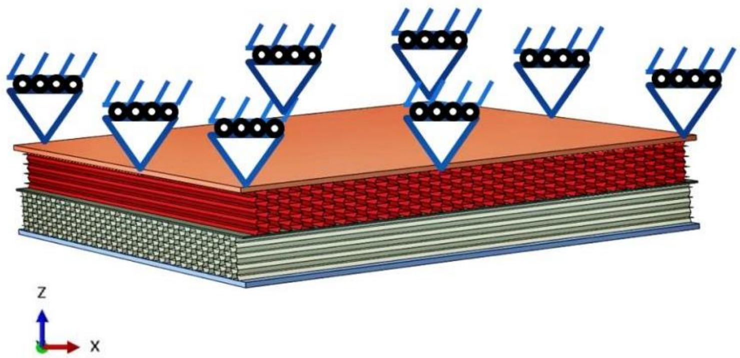

Fig. 2.5 Figure showing the boundary conditions applied to the honeycomb sandwich structure.

Further, in all the simulations pertaining to the sandwiched structure, the structure is considered to be composed of five layers. The first and fifth layers are 3 mm thick plates, referred to as bottom and top plates in the following discussion, while the third layer is 1 mm thick plate. Two layers of 24 mm thick auxetic honeycomb structures, referred to as second and fourth layers, are sandwiched between these plates as shown in Fig. 2.6. Note that the fourth layer is oriented at 90° with respect to the fifth layer to increase symmetry of the structure Further, in the all the simulations of sandwiched structure, the total thickness of structure is taken to be 55 mm, two materials, ceramic and Aluminum for various layers in the structure (refer Fig. 2.6). Thus, three different cases have been considered to understand the effect of material on the blast resistant characteristic of sandwich honeycomb structure. In case 1, all the layers of structure are assumed to be made of aluminum (refer Fig. 2.6 (a)), whereas the entire structure is considered to be made of silicon carbide (ceramic) in case 2 (refer Fig. 2.6 (b)). In the case 3, the bottom and middle plates are assumed to be made of ceramic, while the layers of honeycomb are assumed to be made of aluminum (refer Fig. 2.6 (c)). The figures for all the three cases are given below:

The aluminum and steel components are assumed to follow the Johnson-Cook (J-C) material model, and the J-C damage model described in the previous section, while JH2 model (refer Sec. 2.3) is employed to characterize the deformation behavior of the ceramic. The soil is modeled using the Mohr-Coulomb constitutive theory.

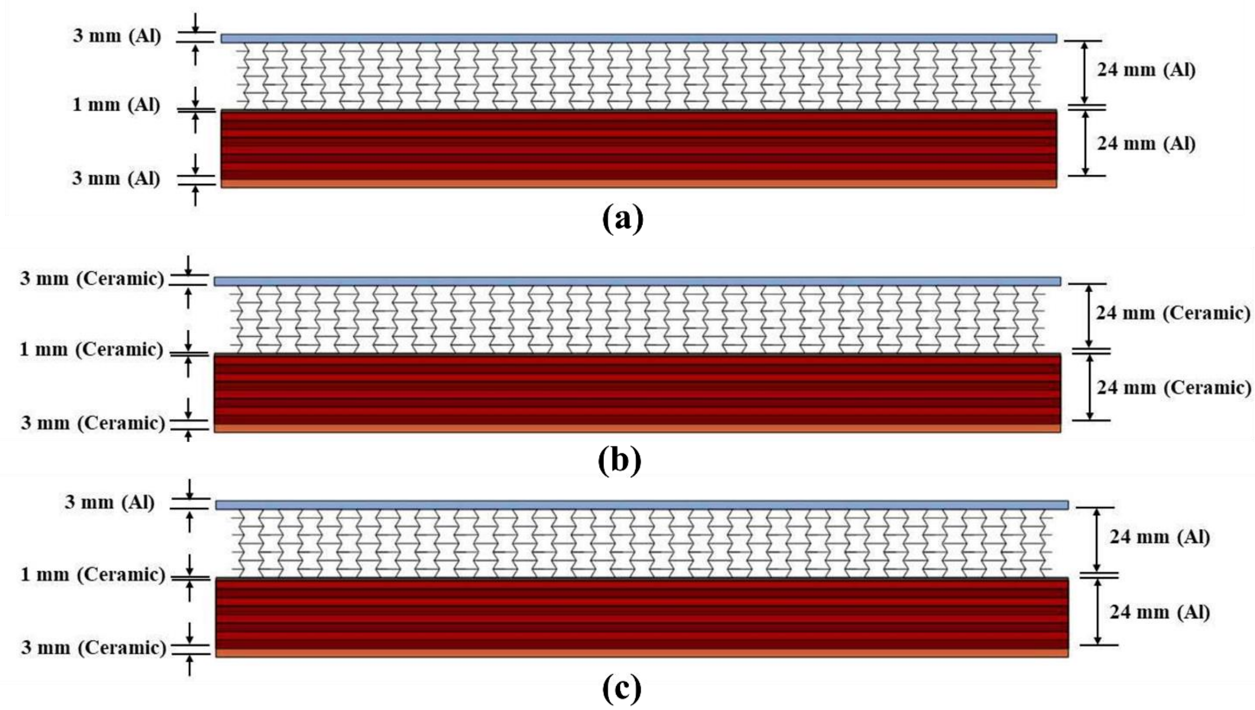

Fig. 2.6 Different structures under considerations for simulating near field blast loading; (a) Case 1, (b) Case 2; (c) Case 3.

2.6 Material properties

The values of material properties for Aluminum [48-50], Silicon carbide [51], Air [52], TNT [53], and Soil [54] are given in the following Tables 1-5, respectively from the page no. 20.

The finite element simulations for the cases discussed in Section 2.5.2 are conducted using CEL technique available with commercially available software package Abaqus 2017. The results from these simulations are thoroughly analyzed and discussed in the subsequent chapter.

Table 1. The values of J-C parameters for Aluminum taken from [48-50].

Aluminum (SI unit)	J-C plastic model	Damage evolution (Fracture energy) 2630009(J/m^3)					
Young Modulus (GPa)			Poisson's ratio				
70			0.3				
A (MPa)	B (MPa)	N	T melt (K)	T transition (K)	M	C	strain rate
520	477	0.52	893	293	1	0.001	0.0005
density (kg/m^3)	d1	$d2$	d3	d4	d5		
2700	0.096	0.049	3.465	0.016	1.099		

Table 2. The values of JH2 parameters for Silicon carbide taken from [51]**.**

Reference density of the material (ρ_o)	3163 kg/m^3	Maximum tensile hydrostatic stress (T)	0.37 GPa	Maximum failure strain $\epsilon_{f\ max}$	1.2
Shear modulus (G)	183 GPa	Maximum normalized intact strength $\sigma_{i\ min}$	1	Bulk modulus (K_1)	204.78 GPa
Intact normalized strength parameter (A)	0.96	Maximum normalized fractured strength $\sigma_{f\ max}$	0.8	Second pressure coefficient (K_2)	0
Intact strength parameter (pressure exponent) (N)	0.65	Net compressive stress at Hugoniot elastic limit (HEL)	14.56 GPa	Third pressure coefficient (K_3)	0
Fractured normalized strength parameter (B)	0.35	Pressure component at the HEL. If not specified, it will be derived from P_{HEL}	5.9 GPa		

Fractured strength parameter (pressure exponent) (M)	1.0	Fraction of elastic energy loss converted to hydrostatic energy (β)	1.0	Failure criteria, FS	0.2
Strength parameter for strain-rate dependence (C)	0.0	Parameter for plastic strain to fracture D_1	0.48		
Reference strain rate $\dot{\epsilon}_o$	1.0	Parameter for plastic strain to fracture (exponent) D_2	0.48		

Table 3. The values of Properties for air taken from [52].

Eos	Air			
Gas Constant (J /kg. K)	Ambient pressure kPa	Specific Heat (J /kg. K)	Dynamic Viscosity (Ns/m^2)	Density (kg/m^3)
287	101	718	1.85×10^{-5}	1.23

Table 4. The values of Properties for TNT taken from [53].

JWL	TNT	C_2(GPa)	R_1
C_d(m/s)	C_1 (GPa)	3.74	4.15
6930	373	W	R2
Density (kg/m^3)	e_o (kJ/m^3)	0.35	0.9
1650	6.06×10^6		

Table 5. The values of Properties for Soil taken from [54].

Eos	Soil					
Elastic modulus (MPa)	Poisson ratio	Friction Angle	Dilation angle	Cohesion Yield stress (MPa)	Abs plastic strain	Density (kg/m^3)
50	0.3	24°	12°	0.1	0.0	2200

Chapter 3

Results and Discussion

The important results obtained from the finite element simulation of the structures subjected to near field blast loading, performed using CEL technique in commercially available software package Abaqus 2017 are discussed in the following subsections.

3.1 Results and discussion

3.1.1 Evolution of deformation in sandwich structure

Figs. 3.1 (a)-(c) show the contour plots of equivalent plastic strain, ϵ^p, at the end of the simulations for sandwich structures pertaining to case-I, II and III, respectively. It can be seen that the aluminum structure deforms in wider and deeper region due its higher ductility (Fig.3.1 (a)), whereas the structure of ceramic shows more localized deformation and fails much earlier in comparison to the aluminum structure. Interestingly, the sandwich structure comprised of first and third layers of ceramics along with aluminum honeycomb and aluminum top plate deform more drastically and uniformly than above two cases. When the blast wave hits the front face sheet, the ceramic starts failing and distributes load on the structure throughout the cross section leading to the more uniform deformation of the structure subjected to near field blast loading.

3.1.2 Evolution of pressure on top surface of structure

The evolution of pressures on top plates of sandwich structure for all three cases is shown in Fig. 3.2. This figure shows that ceramic plate is able to attenuate the pressure effectively; however the pressure rises almost vertically after the failure of ceramic plate. The sandwich structure made of aluminum only performs better than ceramic sandwich structure, but its pressure attenuation capability is poor than the case III structure whereas two plates of ceramic are used. Thus, the present study suggests that use ceramic plate to sandwich aluminum honeycomb is advisable.

3.1.3 Energy absorption in sandwiched structure

Fig.3.3 shows energy absorbed by three sandwich structures under blast loading. It can be seen that integrating ceramic plate to the aluminum honeycomb structure results in longer life of the structure; hence this structure outperforms the sandwich structure made of aluminum only, in terms of energy absorption. The sandwich structure completely made of ceramic fails catastrophically due to brittle nature of silicon carbide and is not able to absorb energy to satisfactory level.

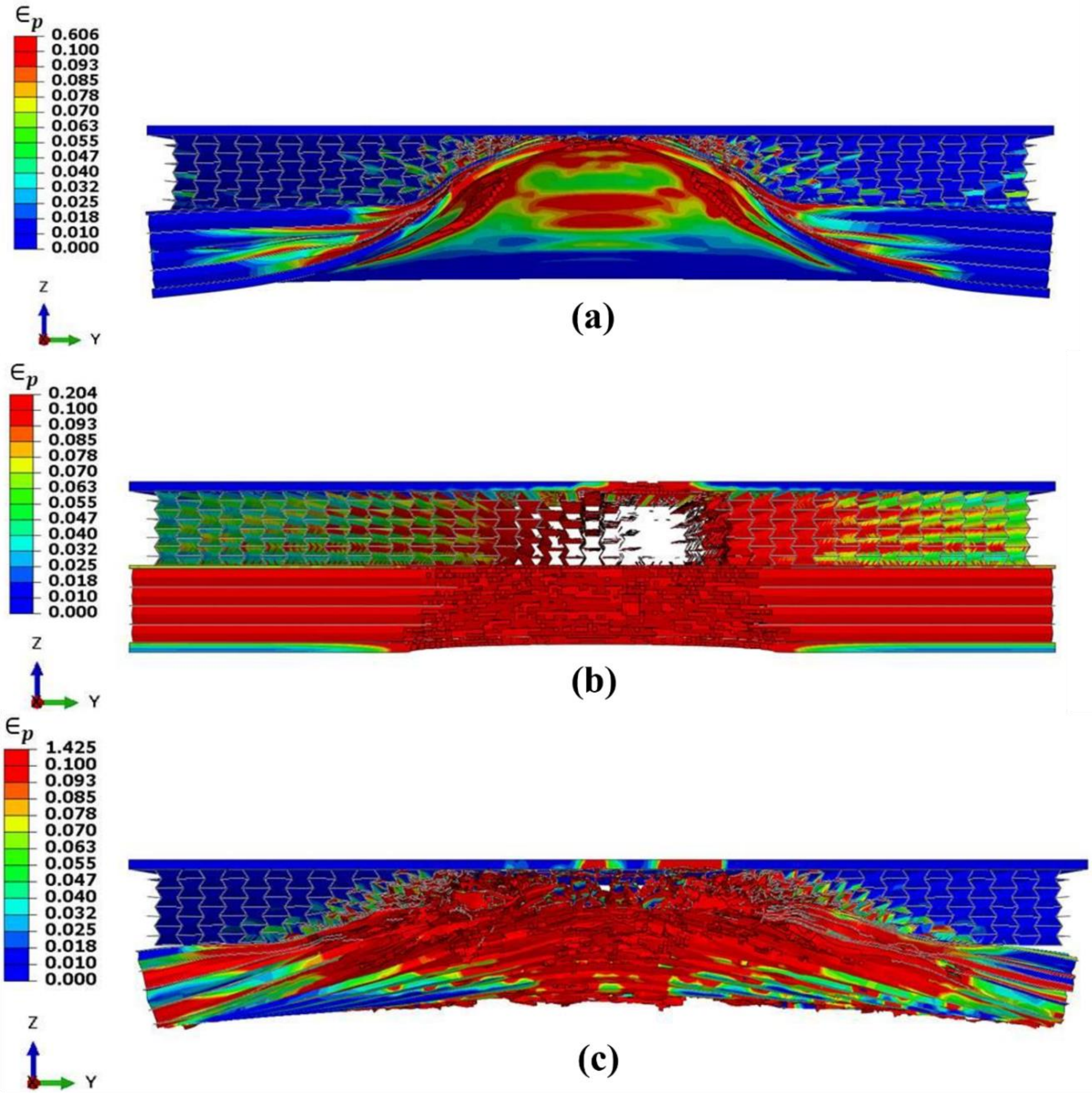

Fig. 3.1 Contour plots of equivalent plastic strain of different sandwich structures under blast loading. (a) Aluminum structure; (b) Ceramic structure; (c) Aluminum honeycomb structure with first and third layers made up of ceramic.

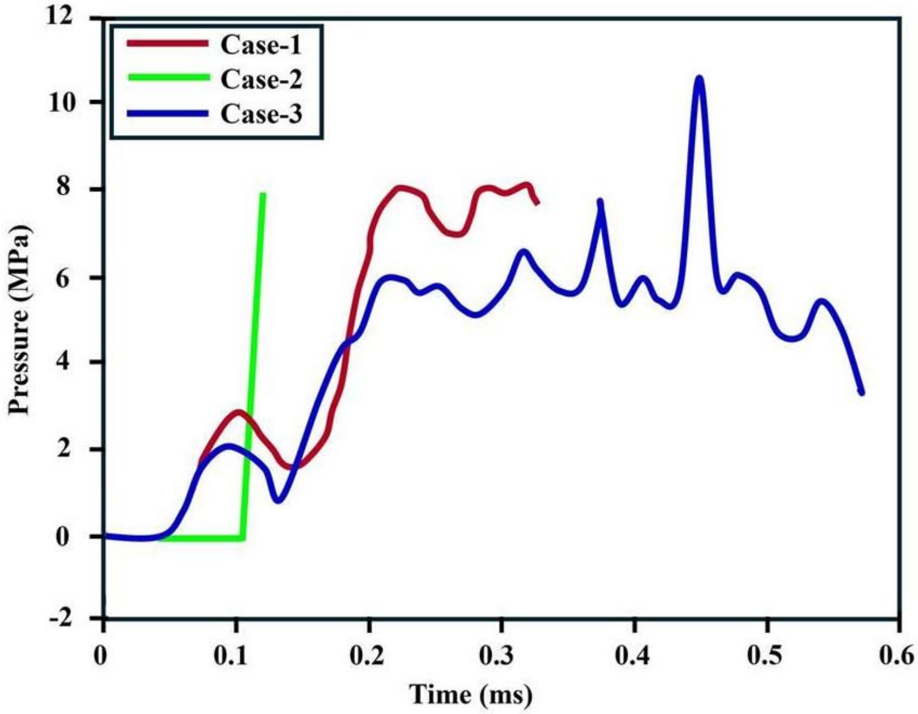

Fig 3.2 Evolution of pressure on the top surface of the structure.

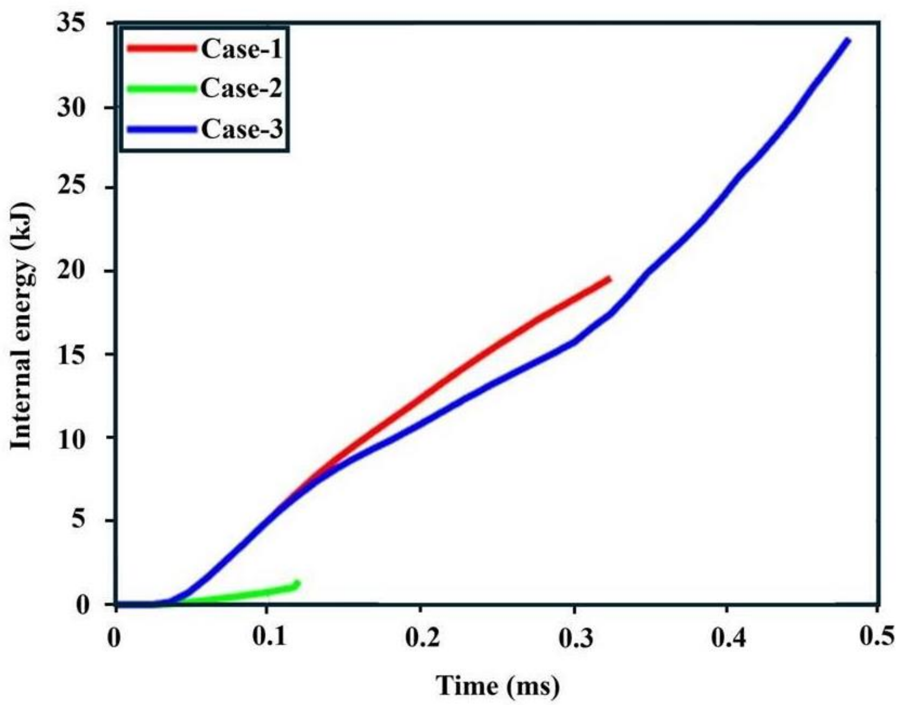

Fig. 3.3 Evolution of energy absorbed by the structure.

3.2 Conclusions

The important conclusions from the previous chapters are summarized below:

- **Deformation behavior**

  The aluminum sandwich structure exhibited extensive deformation over a broader and deeper area due to its higher ductility. In contrast, the ceramic structure showed localized deformation and early failure due to its brittle nature. The composite sandwich structure with ceramic layers and an aluminum honeycomb core demonstrated more uniform deformation. The ceramic layers effectively distributed the blast load across the structure, leading to a more stable deformation pattern under near-field blast conditions

- **Pressure attenuation**

  The aluminum-only sandwich structure performed better in terms of pressure management compared to the ceramic-only structure but was less effective than the composite structure. The composite structure with alternating ceramic and aluminum layers provided the best pressure attenuation; the ceramic plate effectively attenuated the blast pressure initially but after failure of the top aluminum plate, rapid rise in pressure is observed.

- **Energy absorption**

  The composite sandwich structure with ceramic and aluminum layers absorbed the most energy, thereby extending the lifespan of the structure under blast loading. The aluminum-only structure had a moderate energy absorption capability. The ceramic-only structure failed catastrophically and was unable to absorb energy effectively due to the brittle nature of silicon carbide.

In conclusion, the combined structure, which integrates ceramic plates and an aluminum honeycomb core, exhibits the best performance in terms of uniform deformation, pressure attenuation, and energy absorption. This configuration is highly recommended for applications requiring robust blast resistance.

3.3 Future scope

Although the suggested structure is effective and aligns in accordance with the existing literature [8], the experimental evidence is yet to be generated to completely justify the findings of the thesis. Therefore, experiments of blast loading on honeycomb structure with suggested design can be performed in the future.

References

1. https://myanmar-now.org/en/wp-content/uploads/sites/5/2023/09/33QY867-2048x1365.jpg

2. Baker, W.E., 1973. Explosions in air university of texas press. *Austin and London*.

3. Owens, B.D., Kragh, J.F. Jr., Macaitis, J., Svoboda, S.J. and Wenke, J.C. (2007) 'Characterization of extremity wounds in Operation Iraqi Freedom and Operation Enduring Freedom', *Journal of Orthopaedic Trauma*, 21(4), pp. 254-257. https://doi.org/10.1097/bot.0b013e31802f78fb

4. Dougherty, A.L., Mohrle, C.R., Galarneau, M.R., Woodruff, S.I., Dye, J.L. and Quinn, K.H. (2009) 'Battlefield extremity injuries in Operation Iraqi Freedom', *Injury*, 40(7), pp. 772-777. Epub 2009 May 18. PMID: 19450798. https://doi.org/10.1016/j.injury.2009.02.014

5. Fathollahi, S., Yari, A., Fatemi, F., Ardalan, A., Bidarpoor, F. and Esmailnasab, N., 2020. Investigation of health-related consequences of landmine explosions during the past 4 decades (1979-2016): a retrospective cross-sectional study, Kurdistan, Iran. *Disaster medicine and public health preparedness*, *14*(3), pp.322-328. https://doi.org/10.1017/dmp.2019.56

6. Azadi, A., Patnaik, S.S., Jasinski, J.B., Francis, S.L., Lei, Z., Liao, J., Deveneau, N.E. & Ostergard, D.R., 2018. An anatomically-relevant computational model for primary blast effects on the human lower extremity. *Journal of Mechanics in Medicine and Biology*, 18(01), p.1850001. https://doi.org/10.1142/S0219519418500574

7. Dong, L., Zhu, F., Jin, X., Suresh, M., Jiang, B., Sevagan, G., Cai, Y., Li, G., & Yang, K. H. (2013). Blast effect on the lower extremities and its mitigation: A computational study. *Journal of the Mechanical Behavior of Biomedical Materials*, 26, 92-106. https://doi.org/10.1016/j.jmbbm.2013.07.010

8. Neuberger, A., Peles, S. and Rittel, D., 2009. Springback of circular clamped armor steel plates subjected to spherical air-blast loading. *International Journal of Impact Engineering*, *36*(1), pp.53-60. https://doi.org/10.1016/j.ijimpeng.2008.04.008

9. Zhang, C., Wang, Y., Bao, J., Cheng, H., Liu, H., Wang, X., Guo, J. and Li, D., 2023. The anti-explosion performance of ceramic/high-strength steel composite protective

structures. *Journal of Materials Research and Technology*, *24*, pp.7121-7134. https://doi.org/10.1016/j.jmrt.2023.04.265

10. Liu, X.R., Tian, X.G., Lu, T.J. and Liang, B., 2014. Sandwich plates with functionally graded metallic foam cores subjected to air blast loading. *International Journal of Mechanical Sciences*, *84*, pp.61-72. https://doi.org/10.1016/j.ijmecsci.2014.03.021

11. Zhao, C., Zhang, L., Ma, H., Wang, J. and Li, X., 2024. Experimental and numerical study on the blast performance of the corrugated double steel plate concrete composite wallboard under blast loads. *Thin-Walled Structures*, *200*, p.111921. https://doi.org/10.1016/j.tws.2024.111921

12. Thomas, T. and Tiwari, G., 2023. Performance evaluation of Reinforced honeycomb structure under blast load. *Journal of Engineering Research*, *11*(1B). https://doi.org/10.36909/jer.11929 .

13. https://assets.coursehero.com/study-guides/lumen/images/ap1x94x1/the-lower-limbs/left_lower_limb1.png

14. Dharmasena, K.P., Wadley, H.N., Xue, Z. and Hutchinson, J.W., 2008. Mechanical response of metallic honeycomb sandwich panel structures to high-intensity dynamic loading. *International Journal of Impact Engineering*, *35*(9), pp.1063-1074. https://doi.org/10.1016/j.ijimpeng.2007.06.008 .

15. Uth, T. and Deshpande, V.S., 2014. Response of clamped sandwich beams subjected to high-velocity impact by sand slugs. *International journal of impact engineering*, *69*, pp.165-181. https://doi.org/10.1016/j.ijimpeng.2014.02.012 .

16. Kang, D.G., Lehman Jr, R.A. and Carragee, E.J., 2012. Wartime spine injuries: understanding the improvised explosive device and biophysics of blast trauma. *The Spine Journal*, *12*(9), pp.849-857. https://doi.org/10.1016/j.spinee.2011.11.014

17. Yoganandan, N., Stemper, B.D., Pintar, F.A., Maiman, D.J., McEntire, B.J. and Chancey, V.C., 2013. Cervical spine injury biomechanics: applications for under body blast loadings in

military environments. *Clinical Biomechanics*, *28*(6), pp.602-609. https://doi.org/10.1016/j.clinbiomech.2013.05.007

18. Neuberger, A., Peles, S. and Rittel, D., 2009. Springback of circular clamped armor steel plates subjected to spherical air-blast loading. *International Journal of Impact Engineering*, *36*(1), pp.53-60. https://doi.org/10.1016/j.ijimpeng.2008.04.008

19. Zhang, C., Wang, Y., Bao, J., Cheng, H., Liu, H., Wang, X., Guo, J. and Li, D., 2023. The anti-explosion performance of ceramic/high-strength steel composite protective structures. *Journal of Materials Research and Technology*, *24*, pp.7121-7134. https://doi.org/10.1016/j.jmrt.2023.04.265

20. Li, X., Wang, Z., Zhu, F., Wu, G. and Zhao, L., 2014. Response of aluminium corrugated sandwich panels under air blast loadings: experiment and numerical simulation. *International Journal of Impact Engineering*, *65*, pp.79-88. https://doi.org/10.1016/j.ijimpeng.2013.11.002

21. Liu, X.R., Tian, X.G., Lu, T.J. and Liang, B., 2014. Sandwich plates with functionally graded metallic foam cores subjected to air blast loading. *International Journal of Mechanical Sciences*, *84*, pp.61-72. https://doi.org/10.1016/j.ijmecsci.2014.03.021

22. Theobald, M.D., Langdon, G.S., Nurick, G.N., Pillay, S., Heyns, A. and Merrett, R.P., 2010. Large inelastic response of unbonded metallic foam and honeycomb core sandwich panels to blast loading. *Composite structures*, *92*(10), pp.2465-2475. https://doi.org/10.1016/j.compstruct.2010.03.002 .

23. Karagiozova, D., Nurick, G.N., Langdon, G.S., Yuen, S.C.K., Chi, Y. and Bartle, S., 2009. Response of flexible sandwich-type panels to blast loading. *Composites Science and Technology*, *69*(6), pp.754-763. https://doi.org/10.1016/j.compscitech.2007.12.005 .

24. Zhu, F., Zhao, L., Lu, G. and Wang, Z., 2008. Deformation and failure of blast-loaded metallic sandwich panels—experimental investigations. *International Journal of Impact Engineering*, *35*(8), pp.937-951. https://doi.org/10.1016/j.ijimpeng.2007.11.003 .

25. Holmquist, T.J. and Johnson, G.R., 2005. Characterization and evaluation of silicon carbide for high-velocity impact. *Journal of applied physics*, *97*(9). https://doi.org/10.1063/1.1881798 .

26. Qi, C., Yang, S., Yang, L.J., Wei, Z.Y. and Lu, Z.H., 2013. Blast resistance and multi-objective optimization of aluminum foam-cored sandwich panels. *Composite Structures*, *105*, pp.45-57. https://doi.org/10.1016/j.compstruct.2013.04.043 .

27. Bahei-El-Din, Y.A. and Dvorak, G.J., 2008. Enhancement of blast resistance of sandwich plates. *Composites Part B: Engineering*, *39*(1), pp.120-127. https://doi.org/10.1016/j.compositesb.2007.02.006 .

28. Yan, Z., Liu, Y., Yan, J., Wang, B., Bai, F., Shi, Z. and Huang, F., 2022. Anti-blast performance of 3D-printed sandwich panels with auxetic hexagonal and regular hexagonal honeycomb cores. *Engineering Structures*, *272*, p.114996. https://doi.org/10.1016/j.engstruct.2022.114996

29. Zhu, Y., Luo, Y., Gao, D., Yu, C., Ren, X. and Zhang, C., 2022. In-plane elastic properties of a novel re-entrant auxetic honeycomb with zigzag inclined ligaments. *Engineering Structures*, *268*, p.114788. https://doi.org/10.1016/j.engstruct.2022.114788

30. Jin, X., Wang, Z., Ning, J., Xiao, G., Liu, E. and Shu, X., 2016. Dynamic response of sandwich structures with graded auxetic honeycomb cores under blast loading. *Composites Part B: Engineering*, *106*, pp.206-217. https://doi.org/10.1016/j.compositesb.2016.09.037

31. Tang, R.T. and Wen, H.M., 2017. Predicting the perforation of ceramic-faced light armors subjected to projectile impact. *International journal of impact engineering*, *102*, pp.55-61. https://doi.org/10.1016/j.ijimpeng.2016.11.008 .

32. Zhang, X., Zhang, N. and Li, Y., 2011. Numerical study on anti-penetration process of alumina ceramic (AD95) to tungsten long rod *Journal of Modern Physics B*, *25*(15), pp.2091-2103. projectiles. *International* https://doi.org/10.1142/S0217979211100503 .

33. Tasdemirci, A. and Hall, I.W., 2007. Numerical and experimental studies of damage generation in multi-layer composite materials at high strain rates. *International journal of impact engineering*, *34*(2), pp.189-204. https://doi.org/10.1016/j.ijimpeng.2005.08.010 .

34. Krishnan, K., Sockalingam, S., Bansal, S. and Rajan, S.D., 2010. Numerical simulation of ceramic composite armor subjected to ballistic impact. *Composites Part B: Engineering*, *41*(8), pp.583-593. https://doi.org/10.1016/j.compositesb.2010.10.001 .

35. Ning, J., Ren, H., Guo, T. and Li, P., 2013. Dynamic response of alumina ceramics impacted by long tungsten projectile. *International Journal of Impact Engineering*, *62*, pp.60-74. https://doi.org/10.1016/j.ijimpeng.2013.06.006 .

36. Simons, E.C., Weerheijm, J. and Sluys, L.J., 2019. Simulating brittle and ductile response of alumina ceramics under dynamic loading. *Engineering Fracture Mechanics*, *216*, p.106481. https://doi.org/10.1016/j.engfracmech.2019.05.013 .

37. Khan, M.K., Iqbal, M.A., Bratov, V., Morozov, N.F. and Gupta, N.K., 2020. An investigation of the ballistic performance of independent ceramic target. *Thin-Walled Structures*, *154*, p.106784. https://doi.org/10.1016/j.engfracmech.2019.05.013 .

38. Sarvestani, H.Y., Mirkhalaf, M., Akbarzadeh, A.H., Backman, D., Genest, M. and Ashrafi, B., 2019. Multilayered architectured ceramic panels with weak interfaces: energy absorption and multi-hit capabilities. *Materials & Design*, *167*, p.107627. https://doi.org/10.1016/j.matdes.2019.107627

39. Sun, M., Bai, Y., Li, M., Fan, S. and Cheng, L., 2018. Structural design and energy absorption mechanism of laminated SiC/BN ceramics. *Journal of the European Ceramic Society*, *38*(11), pp.3742-3751. https://doi.org/10.1016/j.jeurceramsoc.2018.04.052

40. Karlos, V. and Solomos, G., 2013. Calculation of blast loads for application to structural components. *Luxembourg: Publications Office of the European Union*, *5*. https://dx.doi.org/10.2788/61866

41. Wang, X.H., Zhang, S.R., Wang, C., Cui, W., Cao, K.L. and Fang, X., 2020. Blast-induced damage and evaluation method of concrete gravity dam subjected to near-field underwater explosion. *Engineering Structures*, *209*, p.109996. https://doi.org/10.1016/j.engstruct.2019.109996

42. Johnson, G.R., 1983. A constitutive model and data for metals subjected to large strains, high strain rates and high temperatures. In *Proceedings of the 7th International Symposium on Ballistics, The Hague, Netherlands, 1983*.

43. Johnson, G.R. and Holmquist, T.J., 1994, July. An improved computational constitutive model for brittle materials. In *AIP conference proceedings* (Vol. 309, No. 1, pp. 981-984). American Institute of Physics.https://doi.org/10.1063/1.46199

44. Hu, C. and Zhang, X., 2019. Influence of multiple structural parameters on interior ballistics based on orthogonal test methods. School of Energy and Power Engineering, Nanjing University of Science and Technology, China. https://doi.org/10.1016/0013-7944(85)90052-9

45. Yerro Colom, A., 2015. MPM modelling of landslides in brittle and unsaturated soils. http://dx.doi.org/10.5821/dissertation-2117-102412

46. Cheng, D.S., Hung, C.W. and Pi, S.J., 2013. Numerical simulation of near-field explosion. *Journal of Applied Science and Engineering*, *16*(1), pp.61-67. https://doi.org/10.6180/jase.2013.16.1.09

47. Miller, D., Pan, H., Nance, R., Shirley, A. and Cogar, J., 2010, October. A coupled Eulerian/Lagrangian simulation of blast dynamics. In *Proceedings of the IMPLAST 2010 conference October* (pp. 12-14).

48.Dorogoy, A., Karp, B. and Rittel, D., 2011. A shear compression disk specimen with controlled stress triaxiality under quasi-static loading. *Experimental mechanics*, *51*, pp.1545-1557. https://doi.org/10.1007/s11340-011-9482-3

49. Brar, N.S., Joshi, V.S. and Harris, B.W., 2009, December. Constitutive model constants for Al7075-t651 and Al7075-t6. In *Aip conference proceedings* (Vol. 1195, No. 1, pp. 945-948). American Institute of Physics. https://doi.org/10.1063/1.3295300

50. Børvik, T., Hopperstad, O.S. and Pedersen, K.O., 2010. Quasi-brittle fracture during structural impact of AA7075-T651 aluminium plates. *International journal of impact engineering*, *37*(5), pp.537-551. https://doi.org/10.1016/j.ijimpeng.2009.11.001

51. LeGallic, C., Cauret, M., Tranchet, J.Y., Chartagnac, P., Gil, F., James, B., Pickup, M., Milton, A.L. and Carson, W.A., 1996, September. A consideration of damage in the interaction between tungsten rod penetrators and ceramic materials. In *Proceedings of 16th international symposium on ballistics, San Francisco. CA, USA.*

52. Lemmon, E.W., Jacobsen, R.T., Penoncello, S.G. and Friend, D.G., 2000. Thermodynamic properties of air and mixtures of nitrogen, argon, and oxygen from 60 to 2000 K at pressures to 2000 MPa. *Journal of physical and chemical reference data*, *29*(3), pp.331-385. https://doi.org/10.1063/1.1285884

53. Qasim, M., Kholod, Y., Gorb, L., Magers, D., Honea, P. and Leszczynski, J., 2007. Application of quantum-chemical approximations to environmental problems: Prediction of physical and chemical properties of TNT and related species. *Chemosphere*, *69*(7), pp.1144-1150. https://doi.org/10.1016/j.chemosphere.2007.03.067

54. Lu, G. and Fall, M., 2018. State-of-the-art modelling of soil behaviour under blast loading. *Geotechnical and Geological Engineering*, *36*, pp.3331-3355. https://doi.org/10.1007/s10706-018-0537-5